Available online at www.sciencedirect.com
SCIENCE DIRECT®
Journal of Nuclear Materials 329–333 (2004) 539–543
journal of nuclear materials
www.elsevier.com/locate/jnucmat

Tyranno-SA/SiC composite with SiC nanowires in the matrix by CVI process

W. Yang [a,*], H. Araki [a], A. Kohyama [b], Y. Katoh [b], Q. Hu [a], H. Suzuki [a], T. Noda [a]

[a] *Materials Engineering Laboratory, Micro-nano Component Materials Group, National Institute for Materials Science, 1-2-1 Sengen, Tsukuba 305-0047, Japan*
[b] *Institute of Advanced Energy, Kyoto University, Uji, Kyoto 611-0011, Japan*

Abstract

A SiC nanowire/Tyranno-SA fiber-reinforced SiC/SiC composite was fabricated in situ. Mechanical behaviour during three-point bending were examined. The composite showed marked improvements on the flexural strength and work of fracture compared with a group of conventional Tyranno-SA/SiC composites. Web-like structures, formed from the original SiC nanowires in the composite, were readily observed within the fiber bundles that were not fully deposited with matrix. These web-like structures likely served as reinforcements together with the Tyranno-SA fibers, which provided additional strength and fracture tolerance in the composite.

1. Introduction

Continuous SiC fiber-reinforced SiC matrix composites (SiC/SiC) are advanced candidate structural materials in fusion power plant designs such as TAURO, ARIES, and DREAM because of the radiation resistance, excellent high temperature fracture, creep, corrosion, and thermal shock resistance [1–3]. SiC/SiC composites also possess safety advantages arising from their low induced radioactivity and afterheat. Recently, significant progress has been achieved in the R&D of advanced SiC/SiC composites made with advanced SiC fibers such as Tyranno-SA in terms of baseline properties as well as improved radiation stability [4,5]. Also, SiC/SiC composites have drawn strong interest for aerospace and other applications. Among the several principle challenges for these materials, further improvements of strength and toughness are still important issues.

SiC nanowires have been suggested by Wong et al. [6] as reinforcement materials for ceramic matrix composites to improve strength and toughness, owing to their very high strength over their bulk-counterparts. Wong et al. reported elastic modulus and the largest ultimate bending strength of SiC nanorods were 610–660 and 53.4 GPa, respectively, which are values much higher than those advanced Tyranno-SA and Hi-Nicalon Type-S fibers [7]. Therefore, by incorporating the SiC nanowires in the matrix, SiC/SiC composites with markedly improved strength and toughness might be expected.

In this report, the in situ fabrication and flexural properties of a SiC nanowires/Tyranno-SA fibers-reinforced SiC/SiC composite made by the chemical vapour infiltration (CVI) process with markedly improved strength and fracture tolerance are reported.

2. Experimental

2.1. Growth of SiC nanowires and fabrication of composite

A fibrous preform was prepared from plain-woven Tyranno-SA fiber cloths with a 0/90° layup. The volume

* Corresponding author. Tel.: +81-29 859 2739; fax: +81-29 859 2701.
E-mail address: yang.wen@nims.go.jp (W. Yang).

0022-3115/$ - see front matter © 2004 Elsevier B.V. All rights reserved.
doi:10.1016/j.jnucmat.2004.04.113

load of the fibers was ~43%. Growth of SiC nanowires in situ on the preform Tyranno-SA fibers was carried out with an isothermal CVI system. CH_3SiCl_3 (MTS), was used as the source gas, was carried by hydrogen (H_c) using a standard bubble system. A hydrogen by-pass (H_d) was also used for fine control of the MTS to hydrogen flow ratio. The nanowire growing process was conducted at 1373 K at reduced pressure (1.47 kPa) for 2 h, with 20 and 1000 sccm H_c and H_d flow rates, respectively. The MTS bath temperature was kept at 293 K. After the nanowires growth process was completed, a fabric sheet from the middle of the preform was selected to characterize the synthesized SiC nanowires. Thin carbon layers (from CH_4) were deposited on the Tyranno-SA fibers and SiC nanowires, respectively, by CVI processes before and after the nanowires growth, to modify the fiber/matrix and nanowire/matrix interfacial bondings. The preform was finally CVI-densified with SiC matrix with a volume ratio 1:10 of MTS to carrying gas hydrogen. The densification process continued for 18 h at 1273 K at reduced pressure of 14.7 kPa.

2.2. Mechanical tests

The mechanical properties and fracture behaviours were investigated by the simple three-point bending tests and compared with previous observations [8]. The dimensions of the specimen were $30^{L} \times 4.0^{W} \times 1.5^{T}$ mm^3. Five tests were conducted with a 16 mm support span and with cross-head speed of 0.0083 mm/s.

2.3. Microstructure characterization

The morphology and structure of SiC nanowires were examined with scanning electron microscopy (SEM, JEOL JSM-6700F), high-resolution transmission electron microscopy (HRTEM, JEOL JEM-3000F) and selected area electron diffraction (SAED, JEM-3000F). Energy dispersive spectroscopy (EDS, attached to the JEM-3000F) was used to study the chemistry of the nanowires. The interlayers, microstructures of the composite, and the fracture surfaces were examined using SEM, JSM-6700F.

3. Results and discussion

3.1. SiC nanowires

Successful synthesis of nanowire structures in the fabric sheet was confirmed by SEM examinations, as shown in Fig. 1. The nanowires generally are several tens of microns in length and randomly oriented with straight or curved lengths. Behind the nanowires are the carbon-coated Tyranno-SA fibers. Fig. 2(a) shows that the nanowires are 10–100 nm thick with single cubic β-phase structure (inserted SAED pattern) and possess pure Si–C chemistry (Fig. 2(b)). The volume fraction of the SiC nanowires in the composite preform was estimated by weight gain measurements to be ~5%.

3.2. Composite and flexural properties

The average density and interlayer thickness of the present T-NFRC composite (T stands for Tyranno-SA fiber, NFRC stands for SiC nanowires/fibers-reinforced composite) are given in Table 1. The density was derived from the masses and volumes of the five bending specimens. The PyC (pyrolytic carbon) layer thickness was measured with high magnification SEM images. Several previously fabricated conventional plain-woven CVI-Tyranno-SA/SiC composites [8] are also listed in Table 1 for comparison. The conventional composites in Table 1 were fabricated using the same CVI carbon layer deposition and SiC matrix densification processes as the T-NFRC, except for the SiC nanowires growth process. The reinforcement fibers and their volume fractions are also the same (~43%).

Fig. 3 shows representative flexural stress–displacement curves. The flexural stress was derived from the load–displacement curves using simple beam theory. The composite T-NFRC exhibited several common features with conventional composites upon flexural fracture: (1) an initial linear region, which reflects elastic response of the composites, followed by (2) a nonlinear deformation domain up to the ultimate strength (due mainly to matrix cracking, interfacial debonding and fiber sliding and pullouts, and individual fiber failures), (3) a sudden drop of the stress after the ultimate value is attained, perhaps because of the failure of a significant fraction of the fibers. A residual stress remained until large displacements occurred which depended mainly on the fraction of remaining intact fiber bundles in the specimen. However, composite T-NFRC displayed a

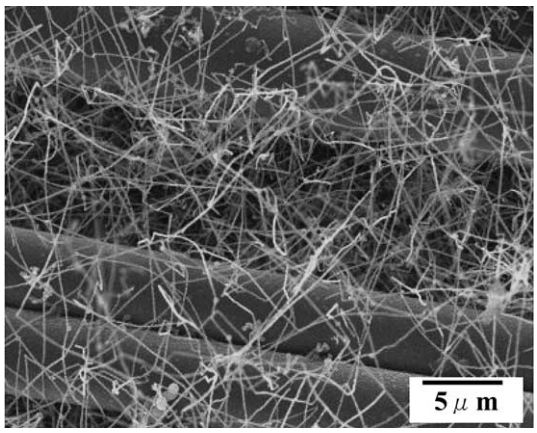

Fig. 1. SiC nanowires on Tyranno-SA fabric sheet.

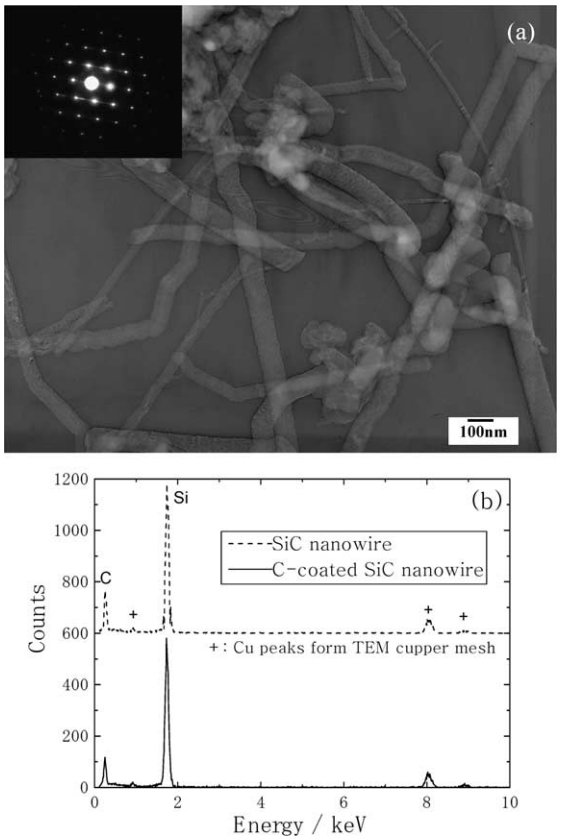

Fig. 2. TEM image and SAED (a) and EDS spectrums (b) of the SiC nanowires.

much larger displacement at ultimate strength (~660 MPa) and a downhill stress ~400 MPa till displacement ~0.4 mm. Fiber pullouts occurred at the fracture surface, as shown in the inserted micrograph. However, debonding and a significant pullout of SiC nanowires were not found at the fracture surfaces, although some broken or fragments of the SiC nanowires were observed by high magnification SEM image examinations.

The flexural properties, including flexural modulus (E_f), proportional limit stress (PLS), and ultimate flexural strength (σ_u), were estimated from the load–displacement curves according to ASTM C 1341-97 [9]. The

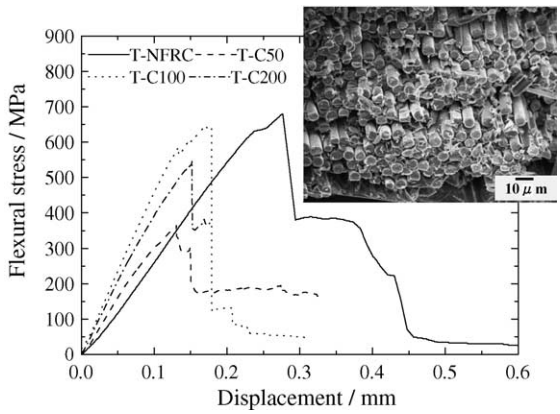

Fig. 3. Typical flexural stress–displacement curves and fiber pullout fracture surface (T-NFRC).

results are given in Table 1. The fracture energies (W_f) were taken as area under the load–displacement curves up to 80% of the load maximums of the decreased loads. For composite T-NFRC, a slightly lower E_f but markedly improved flexural strengths (PLS and σ_u) and W_f were obtained compared with the conventional composites. Among the three conventional composites, T-C100 exhibited the best properties. Compared with this composite, the current T-NFRC showed about 30% and 10% increased PLS and σ_u respectively, and an almost doubled W_f.

3.3. Effect of SiC nanowires

Composite T-NFRC showed marked improvements on the flexural strength and W_f over the conventional SiC/SiC composites. Because the fabrication process were essentially the same for all the composites except for the addition of the SiC nanowires in composite T-NFRC, the markedly improved flexural strength and W_f suggests that the addition of strong SiC nanowires was responsible. After the second carbon layer deposition process, the SiC nanowires were also examined by HRTEM, as shown in Fig. 4. The nanowire cross-section consists of a single crystalline β-SiC core with a thin amorphous shell. High-density stacking faults and microtwins in the crystal plane normal to the axis of the nanowire are clearly shown in

Table 1
Density, interlayer, and flexural properties of composite with SiC nanowires and conventional composites

Composite ID	Density (mg/m^3)	PyC layer (nm)	E_f (GPa)	PLS (MPa)	σ_u (MPa)	W_f (kJ/m^2)
T-NFRC	2.62 ± 0.03	60	120 ± 17	570 ± 120	660 ± 77	6.1 ± 0.7
T-C50[a]	2.41 ± 0.03	50	140 ± 13	260 ± 5	410 ± 92	1.8 ± 0.5
T-C100[a]	2.63 ± 0.04	100	160 ± 11	430 ± 32	610 ± 28	3.2 ± 0.4
T-C200[a]	2.61 ± 0.03	200	140 ± 10	340 ± 18	550 ± 58	2.3 ± 0.3

[a] Previous composites [8].

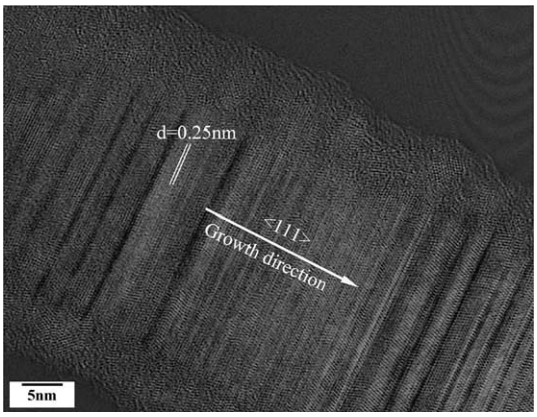

Fig. 4. SiC nanowires with several nanometers carbon coating on the nanowire surface.

the image. The thin amorphous layers on the relatively rough surfaces of the nanowires are carbon from the thermal decomposition of CH_4 because only CH_4 gas was used for the carbon layer deposition. Fig. 4 also shows that the amorphous carbon coating is only several nanometers thick. With such thin carbon coating, the bonding strength between the nanowires and the matrix might be still too strong (considering the relatively rough surfaces of the SiC nanowires and high friction coefficient due to the dens stacking faults) to allow debonding and pullout of the SiC nanowires during fracture procedure. This is the likely reason that pullout of SiC nanowires could not be observed by SEM fracture surface examinations. Although composite T-NFRC with the SiC nanowires exhibited improved the strength, using thicker carbon coatings on the SiC nanowires may enhance composite strength further.

In Fig. 5 micrograph, web-like structures are readily observed composite T-NFRC where the matrix was not fully deposited. Such structures were not found in all the conventional composites in Table 1. These web-like structures likely formed from the clusters of original SiC nanowires in the composite. Pores in SiC/SiC composites, which are inherent with the CVI process, are generally the crack origins during fracture. Often, transverse matrix cracks were observed in SiC/SiC composites that passed through fiber bundles that were not sufficiently infiltrated with matrix, especially for bundles lying perpendicular to the main stress direction in the materials. These web-like structures likely provided additional reinforcement beyond that provided by the Tyranno-SA fibers because of the SiC nanowires connections among the individual fibers in the porous bundles. The much larger W_f of T-NFRC is likely caused by additional nanowire reinforcements in the composite.

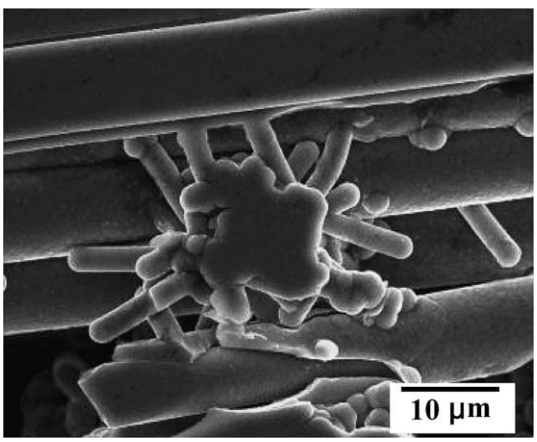

Fig. 5. SiC nanowire web-like structures in insufficiently densified matrix.

4. Conclusion

SiC nanowires were formed via a simple in situ growth directly onto the Tyranno-SA fiber preform prior to the CVI matrix densification of the fiber-reinforced SiC/SiC composite. The volume fraction of the SiC nanowires in the composite was estimated to be ~5%. The composite showed marked improvements on the flexural strength and work of fracture compared with conventional Tyranno-SA/SiC composites.

Pullout of SiC nanowires and debonding/deflection of matrix cracks by the SiC nanowires were rearly observed at the fracture surfaces or in the tested specimens. Apparently, because of the rough nanowire surface characterization, the very thin (several nanometers) carbon coating on the SiC nanowires did not provide sufficiently low bonding strength between the nanowires and the matrix to cause significant debonding and pullout of the SiC nanowires during fracture procedure. However, web-like structures made up of SiC nanowires in the composite were readily observed in the pores within the fiber bundles that were not fully deposited with SiC matrix. These web-like structures apparently provided enough additional reinforcement so that composite flexural strength and fracture tolerance improvements were observed.

Further improvement of the SiC nanowires/Tyranno-SA fibers-reinforced SiC/SiC composite mechanical performance is expected with increased loading of SiC nanowires and/or perhaps better infiltration of the nanowire clusters will improve performance.

Acknowledgements

This study was financially supported by the Budget for Nuclear Research of the Ministry of Education,

Culture, Sports, Science and Technology, based on the screening and counselling by the Atomic Energy Commission.

References

[1] A. Kohyama, M. Seki, K. Abe, T. Muroga, H. Matsui, S. Jitsukawa, S. Matsuda, J. Nucl. Mater. 283–287 (2000) 20.
[2] T. Noda, A. Kohyama, Y. Katoh, Phys. Scr. T91 (2001) 124.
[3] L.L. Snead, O.J. Schwarz, J. Nucl. Mater. 219 (1995) 3.
[4] R.H. Jones, L. Giancarli, A. Hasegawa, Y. Katoh, A. Kohyama, B. Riccardi, L.L. Snead, W.J. Weber, J. Nucl. Mater. 307–311 (2002) 1057.
[5] Y. Katoh, A. Kohyama, T. Hinoki, L.L. Snead, Fusion Sci. Tech. 44 (2003) 155.
[6] E.W. Wong, P.E. Sheenhan, C.M. Lieber, Science 277 (1997) 1971.
[7] A. Hasegawa, A. Kohyama, R.H. Jones, L.L. Snead, B. Riccardi, P. Fenici, J. Nucl. Mater. 283 (2000) 128.
[8] W. Yang, T. Noda, H. Araki, J. Yu, A. Kohyama, Mater. Sci. Eng. A 345 (2003) 28.
[9] ASTM C 1341-97, Standard Test Method for Flexural Properties of Continuous Fiber-reinforced Advanced Ceramic Composites, 2000, p. 509.